

CO Adsorption on Pt(111): From Isolated Molecules to Ordered High-Coverage Structures

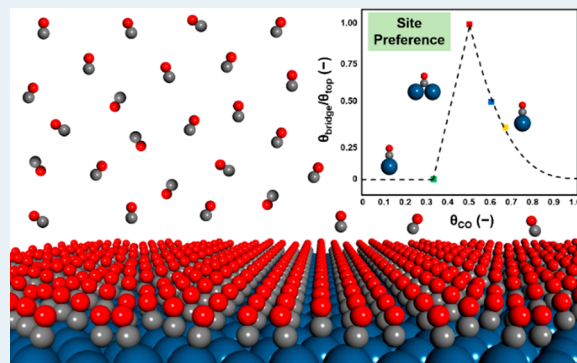
G. T. Kasun Kalhara Gunasooriya^{ID} and Mark Saeys^{*ID}

Laboratory for Chemical Technology, Ghent University, Technologiepark 914, 9052 Gent, Belgium

Supporting Information

ABSTRACT: Carbon monoxide (CO) adsorption on Pt(111) is a bellwether system for surface science, a puzzle for computational catalysis, and a model reaction step in catalysis. While CO can form a nearly infinite number of structures and coverages on Pt(111), only a limited number of ordered structures have been experimentally observed. Here, we used first-principles thermodynamic calculations to evaluate the stability of a few hundred structures for CO on Pt(111), with coverages ranging from 0.06 to 1.0 monolayer. At low coverages, vdW-DF density functional theory calculations confirm the experimentally observed ($\sqrt{3} \times \sqrt{3}$)R30°-CO structure with CO at top sites. At medium coverages, the system switches to the $c(4 \times 2)$ -4CO structure with equal top and bridge site population. The next stable structure is the $c(\sqrt{3} \times 5)$ rect-6CO structure with a bridge:top ratio of 1:2, followed by the $c(\sqrt{3} \times 3)$ rect-4CO structure with a bridge:top ratio of 1:3. This structure corresponds to the saturation coverage under typical reaction conditions. The increase and decrease in the bridge:top ratio with coverage, from 0 to 1:1 and back to 0, is correctly predicted by vdW-DF and is driven by the change in the Pt surface charge upon CO adsorption at top and bridge sites.

KEYWORDS: catalysis, density functional theory, platinum, CO adsorption, coverage



1. INTRODUCTION

Carbon monoxide (CO) adsorption on transition-metal surfaces is an important elementary reaction in CO oxidation,^{1–3} the water-gas shift reaction,^{4,5} and Fischer-Tropsch synthesis.^{6–9} Adsorption of CO on platinum surfaces has received continued interest ever since Irving Langmuir studied this system,¹⁰ and CO adsorption on platinum is considered a prototype system in the field of surface science and computational catalysis.¹¹ While CO can in principle form a nearly infinite number of structures and coverages on Pt(111), adsorbing on top, bridge, and hollow sites, only a limited number of ordered structures have been experimentally observed: namely, ($\sqrt{3} \times \sqrt{3}$)R30°-CO, $c(4 \times 2)$ -4CO, $c(\sqrt{3} \times 5)$ rect-6CO, $c(\sqrt{3} \times 3)$ rect-4CO. Interestingly, other ordered structures, such as ($\sqrt{7/3} \times \sqrt{7/3}$)R10.9°-3CO and ($2\sqrt{3} \times 2\sqrt{3}$)R30°-7CO, which are observed on Co(0001)¹² and Ru(0001)¹³ at medium to high CO coverages, are not observed on Pt(111). In these ordered structures, CO can adsorb at top, bridge, and hollow sites and with a different number of CO molecules per unit cell. While the ordered periodic unit cell is often easy to determine experimentally, the ratio between bridge and top CO is more challenging to measure. For example, for the $c(\sqrt{3} \times 5)$ rect-6CO unit cell, structures with different bridge:top ratios and with different CO locations in the $c(\sqrt{3} \times 5)$ rect unit cell have been proposed.^{14–16}

Thermodynamic calculations based on density functional theory (DFT) provide a tool to compare the relative stabilities of hundreds of possible structures in different unit cells for CO on Pt(111) and to identify the most stable structures as a function of the CO pressure and temperature. Unfortunately, the accurate calculations of the site preference and of the adsorption energy of CO on Pt(111) remain important challenges for DFT; this challenge was famously coined “the CO/Pt(111) Puzzle”.^{17–21} While a large number of DFT studies have considered low-coverage CO adsorption on Pt(111), only a limited number of studies investigated kinetically relevant higher coverages.^{22–24} Hafner et al.²² studied CO adsorption in partially precovered $c(\sqrt{3} \times 2)$ rect and $c(\sqrt{3} \times 3)$ rect unit cells for a selected number of high-coverage CO adsorption structures, while Shan et al.²³ reported coverage-dependent CO adsorption energies for CO adsorption in a $p(4 \times 4)$ unit cell with 0.25, 0.5, 0.75, and 1.0 ML coverage.

We recently showed that calculations with the vdW-DF functional accurately describe CO adsorption on Pt(111) and that the relative stabilities of different structures in a given unit cell are correctly calculated.²⁵ In the present work, we use the selected method to evaluate the stability of a few hundred

Received: June 19, 2018

Revised: September 18, 2018

Published: September 21, 2018

possible structures and identify the most stable structures as a function of the CO pressure and temperature. First, a brief overview of important experimental studies of CO adsorption on Pt(111) is provided. Next, the stability for CO is evaluated for low, medium, and high coverage using $p(3 \times 3)$, $c(4 \times 2)$, and $c(\sqrt{3} \times 5)\text{rect}$, $c(\sqrt{3} \times 3)\text{rect}$, and $(2\sqrt{3} \times 2\sqrt{3})\text{R}30^\circ$ unit cells, respectively. Gibbs free energy calculations are used to determine the equilibrium CO coverage and the dominant structure as a function of the CO chemical potential. Finally, the variation in the bridge:top ratio as a function of the CO coverage is discussed.

2. BRIEF OVERVIEW OF EXPERIMENTAL STUDIES FOR CO ADSORPTION ON Pt(111)

A wide range of experimental techniques, such as low energy electron diffraction (LEED), temperature-programmed desorption (TPD), work function measurements, electron energy loss spectroscopy (EELS), molecular beam scattering, reflection-absorption infrared spectroscopy (RAIRS), X-ray photoemission spectroscopy (XPS), calorimetry, and scanning tunneling microscopy (STM), have been used to study the adsorption of CO on platinum surfaces.^{14,26–38} From this body of work, a sequence of stable ordered structures with increasing CO coverage have been determined.

In the limit of zero coverage, an adsorption energy of -130 ± 3 kJ/mol is determined by single-crystal adsorption calorimetry,³⁹ although early calorimetric studies on thin films have determined a rather high value of 183 kJ/mol.^{36,40} Work function²⁸ and TPD³⁰ measurements lead to experimental heats of adsorption of -138 ± 8 and -145 ± 15 kJ/mol, respectively. At low coverages, CO preferably adsorbs at top sites and a single sharp IR peak near 2100 cm^{-1} is observed.^{28,30} At low coverages, LEED studies at 300 K and for an exposure of 1 L show a rather diffuse $(\sqrt{3} \times \sqrt{3})\text{R}30^\circ$ -1CO diffraction pattern with CO at top sites (Figure 1).^{14,28} At

coverage, three different models have been proposed for the $c(\sqrt{3} \times 5)\text{rect}$ -6CO structure (Figure 2). In the structure proposed by Persson et al.¹⁵ and in the structure proposed by Avery,¹⁴ the bridge:top ratio is 1:2, but the location of the top CO differs. On the basis of a reassessment of published LEED patterns, Petrova and Yakovkin¹⁶ proposed a structure with a bridge:top ratio of 2:1. However, the structure proposed by Petrova and Yakovkin is not consistent with the bridge:top ratio obtained from EELS¹⁴ and XPS⁴² data.

The next stable structure has a coverage of 0.67 ML and a $c(\sqrt{3} \times 3)\text{rect}$ -4CO unit cell. On the basis of LEED and HREELS studies, Avery¹⁴ proposed a structure with a bridge:top ratio of 1:3 (Figure 3). Biberian and Van Hove,³² using LEED and TPD, proposed a structure with a bridge:top ratio of 3:1. A structure with equal population of bridge and top sites can also be drawn.

3. COMPUTATIONAL METHODS

CO adsorption on Pt(111) was studied using periodic density functional theory with the vdW-DF^{43,44} functional, a plane-wave basis set with a cutoff kinetic energy of 450 eV, and the projector-augmented wave method as implemented in the Vienna ab-initio simulation package (VASP).^{45,46} For comparison, PBE⁴⁷ calculations are reported as well. The Pt(111) surface was modeled as a five-layer slab. On the basis of the surface science data discussed in the previous section, a limited number of unit cells were used for the calculations, but the number of CO molecules per unit cell and their adsorption sites (top and bridge) were extensively sampled. Though machine learning or cluster expansions could automate the search, the symmetry of the configurations allowed us to manually sample the high-coverage structures. In particular, we used $p(4 \times 4)$, $p(3 \times 3)$, $c(4 \times 2)$, $c(\sqrt{3} \times 2)\text{rect}$, $(2\sqrt{3} \times 2\sqrt{3})\text{R}30^\circ$, $c(\sqrt{3} \times 5)\text{rect}$, and $c(\sqrt{3} \times 3)\text{rect}$ unit cells to evaluate the adsorption of CO. To obtain numerically converged results, the Brillouin zone was sampled with $(3 \times 3 \times 1)$, $(3 \times 3 \times 1)$, $(3 \times 5 \times 1)$, $(5 \times 5 \times 1)$, $(3 \times 3 \times 1)$, $(5 \times 3 \times 1)$, $(5 \times 3 \times 1)$ Monkhorst–Pack grids, respectively, for the different unit cells. The bottom two layers were constrained at the bulk positions with optimized lattice constants of 4.028 (vdW-DF) and 3.977 (PBE) Å (experimental value 3.912 Å⁴⁸), while the top three layers and the adsorbed CO molecules were fully optimized. An interlayer spacing of 15 Å was found to minimize interactions between repeated slabs. All the geometries were optimized until the energy between consecutive steps changed by less than 0.1 kJ/mol. Dipole corrections were accounted for as implemented in VASP.⁴⁹

To evaluate the thermodynamic stability of the different structures as a function of pressure and temperature, Gibbs free adsorption energies, $\Delta G_{\text{ads}}(T,p)$, were calculated with reference to a gas-phase reservoir of CO (eq 1⁵⁰).

$$\Delta G_{\text{ads}}(T,p) = \Delta G^\circ(T) - RT \ln p_{\text{CO}} \quad (1)$$

Gibbs free energies for gas-phase CO and for the various surface structures were obtained by combining the electronic and zero-point energies with enthalpy and entropy corrections from frequency calculations for the full structure (Supporting Information, Table S8) and using the harmonic oscillator (HO) approximation. Since the CO diffusion barriers are at least 5 kJ/mol at low coverage and are higher at high coverage, the HO approximation remains valid for the entropy

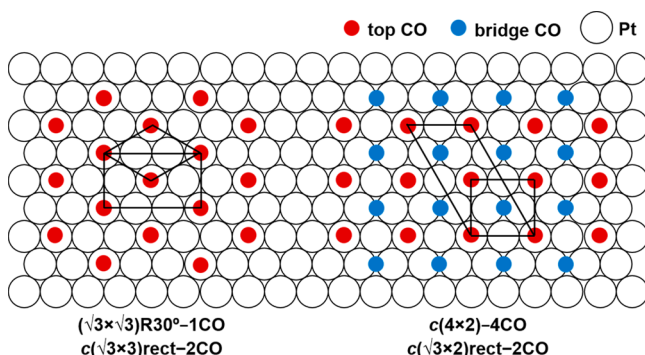


Figure 1. Low- and medium-coverage ordered structures for CO on Pt(111). At low coverage, a $(\sqrt{3} \times \sqrt{3})\text{R}30^\circ$ -1CO or $c(\sqrt{3} \times 3)\text{rect}$ -2CO structure with CO at top sites has been reported, while at 0.5 ML, a $c(4 \times 2)$ -4CO or $c(\sqrt{3} \times 2)\text{rect}$ -2CO configuration with equal population of bridge and top CO has been observed.

half-monolayer coverage, LEED shows a well-ordered $c(4 \times 2)$ -4CO or $(\sqrt{3} \times 2)\text{rect}$ -2CO pattern (Figure 1) below 300 K.³⁰ At this coverage, IR spectra indicate the presence of both top and bridge CO.^{14,32} EELS,^{29,30} He scattering,⁴¹ and XPS⁴² indicate that the bridge and top sites are equally populated at this coverage.

For coverages beyond 0.5 ML, several ordered structures have been reported. The next stable coverage is 0.6 ML. At this

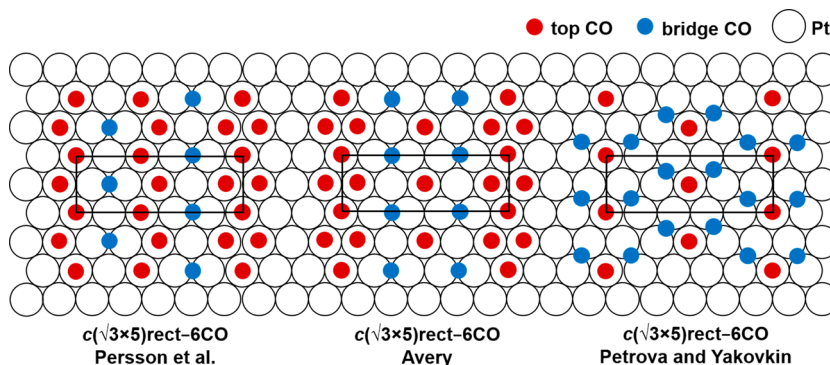


Figure 2. 0.6 ML ordered $c(\sqrt{3} \times 5)\text{rect}-6\text{CO}$ structures proposed for CO on Pt(111). The structures proposed by Persson et al.¹⁵ and Avery¹⁴ have a bridge:top ratio of 1:2, while the structure proposed by Petrova and Yakovkin¹⁶ has a bridge:top ratio of 2:1.

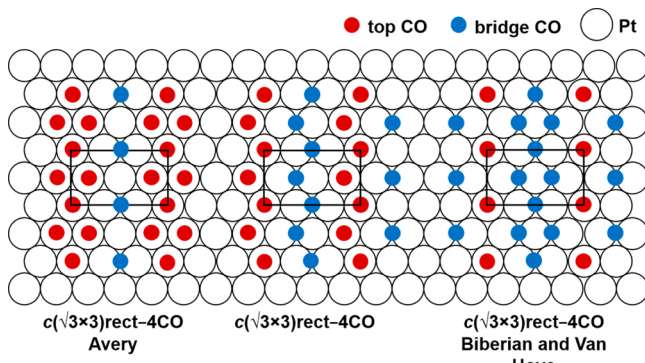


Figure 3. 0.67 ML ordered $(\sqrt{3} \times 3)\text{rect}-4\text{CO}$ structures proposed for CO on Pt(111). The structure proposed by Avery¹⁴ has a bridge:top ratio of 1:3, while the structure proposed by Biberian and Van Hove has a bridge:top ratio of 3:1. A structure with equal occupancy of the top and bridge sites is added for completion.

calculation.⁵¹ The effect of using phonon spectra instead of HO frequencies on the relative stability was found to be limited (Supporting Information, Table S1). Six frequencies were used per CO to determine the entropy corrections (Supporting Information, Figure S2): the typical CO stretching frequency and five low-frequency modes associated with Pt–C stretching, frustrated rotation, and translation, with frequencies in the range of 50–500 cm⁻¹. Frequencies below 50 cm⁻¹ have a large effect on the calculated adsorption entropy. Changing such a frequency from 50 to 40 cm⁻¹ results in a 2 J/(mol K) change in the entropy at 300 K. To construct the first-principles stability diagram, the Gibbs free adsorption energy per surface Pt atom, i.e., $\theta_{\text{CO}}\Delta G_{\text{ads}}(T,p)$, was calculated as a function of the CO chemical potential (μ_{CO}).

4. RESULTS AND DISCUSSION

4.1. Low-Coverage Structures. Table 1 summarizes the optimized structures and the corresponding adsorption energies for CO adsorption in a $p(3 \times 3)$ unit cell with coverages of 1/9, 2/9, and 1/3 ML. Several combinations of bridge and top adsorption are considered. The vdW-DF calculations correctly predict the preference for the top site at low CO coverages, and the adsorption energy of -147 to -142 kJ/mol is close to the experimental range, -130 to -145 kJ/mol.^{28,30,39} At 300 K and 1 mbar, the adsorption Gibbs free energy is very favorable at -80 kJ/mol, and even at 1 mbar the temperature needs to increase to 676 K to favor desorption (eq 1). As expected, the PBE functional overestimates the strength

of CO adsorption by 30–40 kJ/mol and favors the hollow site.^{17–21}

The calculations show that the CO adsorption Gibbs free energy at the bridge sites is 5 kJ/mol less stable than at the top site. Experimentally, the bridge sites are 4 kJ/mol less stable than the top sites at low CO coverage.⁵² Hollow sites are even less stable on Pt(111). The preference for the bridge sites over the hollow sites on Pt(111) agrees with experimental data, but this relative stability depends on the transition metal. For example on Co(0001), CO adsorption at the bridge site is 4 kJ/mol less stable than adsorption at the hollow site.⁵³ CO adsorption at hollow sites is hence not observed on Pt(111), while it has been reported experimentally for high-coverage structures on Co(0001).^{53,54} The entropy for CO at the top site is 4 J/(mol K) higher than for CO on the bridge and hollow sites. This higher entropy results from a higher frustrated translational entropy of 34 J/(mol K) in comparison to 29 J/(mol K) for the bridge site (Supporting Information, Table S8 for vibrational frequencies). Despite the stronger adsorption, CO is hence slightly more mobile at the top site.

Several configurations of CO at the bridge and top sites were considered for two and three CO molecules, and the most stable configurations for 2T, 1T+1B, and 2B and for 3T, 2T+1B, and 3B are shown in Table 1. In addition, for two and three CO molecules per unit cell, adsorption at the top sites remains preferred in the vdW-DF calculations, but the difference in stability between the top and bridge sites decreases from 5 kJ/mol for the first CO to 2 kJ/mol for the second CO and only 1 kJ/mol for the third CO. At 1/3 ML coverage, the $(\sqrt{3} \times \sqrt{3})R30^\circ$ -CO structure with CO at top sites is the most stable structure, in agreement with experiments.^{28,30,32} The CO adsorption energy decreases by 5 kJ/mol when the coverage increases from 1/9 to 1/3 ML, and the interaction between neighboring CO molecules is hence slightly repulsive. For a coverage of 1/3 ML, PBE incorrectly predicts the $(\sqrt{3} \times \sqrt{3})R30^\circ$ -CO structure with CO at hollow sites as the most stable structure (Supporting Information, Table S2).

4.2. Medium-Coverage Structures. Table 2 summarizes calculations for 3/8 and 1/2 ML CO coverage. Different combinations of bridge and top adsorption for one, two, three, and four CO molecules were considered in the $c(4 \times 2)$ unit cell (Table 2 and Supporting Information, Table S3). Adsorption at the hollow sites was not considered for medium and high coverages. At 3/8 ML coverage, the vdW-DF functional predicts that the 2T+1B configuration is the most stable, while the PBE functional favors the 1T+2B config-

Table 1. CO Adsorption Energies (kJ/mol), Gibbs Free Adsorption Energies (300 K, 1 mbar CO; kJ/mol), and Average Entropies of Adsorbed CO (J/(mol K)) for Different Low-Coverage Configurations in a $p(3 \times 3)$ Unit Cell on Pt(111)^a

Functional	1/9 – 1T	1/9 – 1B	1/9 – 1H
vdW-DF	-147/-80/46	-143/-75/42	-139/-72/41
PBE	-174/-106/46	-181/-113/41	-182/-113/37
vdW-DF	-145/-77/48	-144/-76/45	-142/-74/42
PBE	-171/-102/45	-176/-107/43	-178/-109/41
vdW-DF	-142/-74/48	-141/-73/46	-138/-70/42
PBE	-167/-99/46	-171/-102/44	-174/-105/40

^aThe most stable configuration for the vdW-DF and for the PBE functional is indicated. Abbreviations: T, top; b, bridge; h, hollow.

Table 2. Average CO Adsorption Energies (kJ/mol), Average Gibbs Free Adsorption Energies (300 K, 1 mbar CO; kJ/mol) and Average Entropies of Adsorbed CO (J/(mol K)) for Different Medium-Coverage Configurations in a $c(4 \times 2)$ Unit Cell^a

Functional	3/8 – 3T	3/8 – 2T+1B	3/8 – 1T+2B
vdW-DF	-135/-68/49	-141/-73/45	-138/-70/43
PBE	-161/-92/46	-169/-100/44	-171/-101/41
vdW-DF	-127/-60/49	-135/-67/46	-139/-70/43
PBE	-158/-89/47	-161/-92/44	-168/-98/41

^aThe most stable configuration for each coverage is indicated. Abbreviations: T, top; b, bridge.

uration. At 1/2 ML, the most stable structure has an equal population of top and bridge sites, in agreement with XPS, RAIRS, EELS, and LEED data.^{29–31,33,41,42} At 300 K and 1 mbar, the average Gibbs adsorption free energy remains very favorable, -70 kJ/mol. The structure with all CO at top sites is

10 kJ/mol less stable, while the structure with all CO at bridge sites (Supporting Information, Table S3) is 17 kJ/mol less stable than the mixed structure.

4.3. High-Coverage Structures. Three different configurations have been proposed for the $c(\sqrt{3} \times 5)\text{rect}$ -6CO

Table 3. Average CO Adsorption Energies (kJ/mol), Average Gibbs Free Adsorption Energies (300 K, 1 mbar; kJ/mol), and Entropies of Adsorbed CO (J/(mol K)) for Different Combinations of Six CO Molecules at Bridge and Top Sites in a $c(\sqrt{3} \times 5)$ rect Unit Cell (6/10 ML) and of Four CO Molecules in a $c(\sqrt{3} \times 3)$ rect Unit Cell (4/6 ML)^a

$c(\sqrt{3} \times 5)$ rect unit cell			
Functional	6/10 – 4T + 2B (Persson et al.)	6/10 – 4T + 2B (Avery)	6/10 – 2T + 4B (Petrova and Yakovkin)
vdW-DF	-134/-65/42	-132/-63/42	-124/-55/41
PBE	-158/-89/41	-157/-87/40	-157/-86/39
$c(\sqrt{3} \times 3)$ rect unit cell			
Functional	4/6 – 3T+1B (Avery)	4/6 – 2T+2B	4/6 – 1T+3B (Biberian and Van Hove)
vdW-DF	-127/-57/40	-123/-53/40	Not stable.
PBE	-149/-79/39	-148/-78/39	Not stable.

^aThe most stable configuration for each coverage is indicated. Abbreviations: T, top; B, bridge.

Table 4. Average CO Adsorption Energies (kJ/mol), Average Gibbs Free Adsorption Energies (300 K, 1 mbar CO) (kJ/mol), and Average Entropies of Adsorbed CO (J/(mol K)) for the Most Stable Configurations of Five and Eight CO Molecules in a $c(4 \times 2)$ Unit Cell and for Seven CO Molecules in a $(2\sqrt{3} \times 2\sqrt{3})R30^\circ$ Unit Cell^a

Functional	5/8 – 3T+1H+1F	7/12 – 1T+6B	1 – 8T
vdW-DF	-129/-60/41	-131/-62/40	-77/-4/31
PBE	-150/-81/39	-167/-97/39	-96/-23/31

^aAbbreviations: T, top; b, bridge; H, hollow-hcp; F, hollow-fcc.

structure (Table 3). The structures proposed by Avery¹⁴ and by Persson et al.¹⁵ have four top and two bridge CO molecules per unit cell (0.6 ML) but differ in the relative location of the molecules. The structure proposed by Petrova and Yakovkin¹⁶ has four bridge and two top CO molecules per unit cell. PBE calculations fail to identify a dominant structure, artificially overestimating the structure with a higher bridge coverage. vdW-DF calculations clearly favor the structures with a bridge:top ratio of 1:2, in agreement with quantitative XPS data,⁴² and show a slight preference of 2 kJ/mol of CO for the structure proposed by Persson et al. While it would be interesting to use the computed vibrational frequencies and intensities for the three structures to help identify the experimentally observed structure, the difference in the calculated frequencies is too small to allow such an identification (Supporting Information, Table S8).

The next experimentally observed ordered structure is $c(\sqrt{3} \times 3)$ rect-4CO (Table 3 and Supporting Information, Table S6). For this coverage, structures with only top and only bridge CO could not be converged. The most stable configuration has three top and one bridge CO and corresponds to the structure proposed by Avery.¹⁴ As shown below, this coverage corresponds to the saturation coverage on Pt(111) at typical pressures and temperatures. The calculated adsorption energy, -127 kJ/mol, is comparable to values obtained by calorimetry for a saturated Pt(111) surface, -118 kJ/mol.⁵⁵ PBE again favors a structure with a higher bridge:top ratio and overpredicts the adsorption energy. The structure proposed by Biberian and Van Hove with a high bridge:top ratio of 3:1 could not be converged. In the preferred structure, two of the three CO molecules at the top sites tilt away from the surface normal by 14°. Using electron stimulated desorption ion angular distributions (ESDIAD), Kiskinova et al.³⁴ observed

tilting of the top CO molecules with a tilting angle of $14 \pm 1^\circ$ for CO coverages above 0.6 ML on Pt(111). The tilting likely minimizes through-space repulsion. A similar tilting for CO adsorbed at top sites was observed for the structures proposed by Avery¹⁴ and by Persson et al.¹⁵ at 0.6 ML coverage corresponding to the $c(\sqrt{3} \times 5)$ rect-6CO structure (Table 3).

We also evaluated structures with five CO molecules in a $c(4 \times 2)$ unit cell ($5/8$ ML), eight molecules in a $c(4 \times 2)$ unit cell (1 ML), and seven molecules in a $(2\sqrt{3} \times 2\sqrt{3})R30^\circ$ unit cell ($7/12$ ML) (Table 4). The $5/8$ ML structure is interesting, since both PBE and vdW-DF converge to a structure with two CO molecules at hollow sites and three at top sites. The preference for the hollow sites minimizes through-space repulsion. Combinations with CO at the bridge and the top sites were not stable. The differential adsorption energy for the additional CO molecule in the unit cell is rather low, however, -123 kJ/mol. At sufficiently high CO pressure and low temperature, the $(2\sqrt{3} \times 2\sqrt{3})R30^\circ$ -7CO structure ($7/12$ ML) has been observed on Ir(111),⁵⁶ Co(0001),¹² and Ru(0001).¹³ In this structure, CO adsorbs at top and bridge sites with a high bridge:top ratio of 6:1. On Pt(111) as well, this is the most stable structure for seven CO molecules in a $(2\sqrt{3} \times 2\sqrt{3})R30^\circ$ unit cell (Table 4), with a high average CO adsorption energy of -131 kJ/mol. We will show below that the $c(4 \times 2)$ -5CO and the $(2\sqrt{3} \times 2\sqrt{3})R30^\circ$ -7CO structures are not the most stable structures for any value of the CO chemical potential and, in agreement, they are therefore not observed experimentally.

Monolayer CO coverage was studied in a $c(4 \times 2)$ unit cell. At this coverage, CO adsorbs at the top site (Table 4). The structure with CO at the bridge sites is 20 kJ/mol less stable (Table S3). Mixed structures with different ratios of bridge and top sites could not be converged. The CO adsorption energy remains quite strong at 1 ML, -77 kJ/mol, and the average Gibbs adsorption free energy at 300 K and 1 mbar, -4 kJ/mol, suggests that ML coverages are achievable on Pt(111). Increasing the CO pressure to 1 bar makes the monolayer structure even more stable, -21 kJ/mol. We will show below, however, that this conclusion is misleading, as the differential adsorption free energy, and not the average adsorption free energy, determines whether the coverage can be increased. The entropy of adsorbed CO, 31 J/(mol K) at the top sites, is significantly lower than the low-coverage value, 46 J/(mol K), reflecting the increased frequencies for the frustrated translational modes at high coverage.

4.4. Comparison of the Stabilities of the Various Structures. To compare the stability of the many structures that were discussed above and in the Supporting Information, and to identify stable structures as a function of the CO chemical potential, the Gibbs adsorption free energy per Pt atom, $\theta_{CO}\Delta G_{ads}(T,p)$, is plotted as a function of the CO chemical potential in Figure 4. Only the most stable structure for each coverage is included in Figure 4. For very low values of CO chemical potential, the clean Pt(111) surface is the most stable. As the CO chemical potential increases, CO adsorbs gradually at the top sites up to a coverage of $1/3$ ML to form an ordered $(\sqrt{3} \times \sqrt{3})R30^\circ$ -CO structure. The next stable ordered structure is the $c(4 \times 2)$ -4CO structure, where CO adsorbs at both top and bridge sites. The structure with an intermediate coverage, $c(4 \times 2)$ -3CO ($3/8$ ML), is not stable for any value of the CO chemical potential. Another ordered structure with intermediate coverages, $p(4 \times 4)$ -7CO (Supporting Information, Table S7), is also not stable for

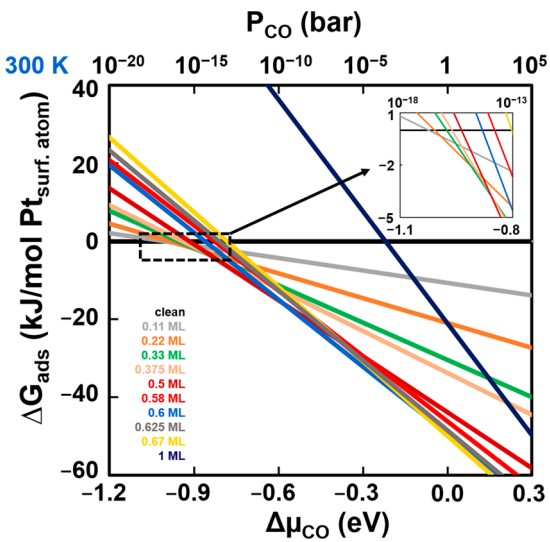


Figure 4. Gibbs free adsorption energy per Pt atom, $\theta_{CO}\Delta G_{ads}(T,p)$ (kJ/mol of Pt surface atoms) as a function of the CO chemical potential (μ_{CO}) for the most stable structure for every coverage considered. The chemical potential is also converted to the CO pressure at 300 K. The following structures were considered: 0.11 ML, $p(3 \times 3)$ -CO; 0.22 ML, $p(3 \times 3)$ -2CO; 0.33 ML, $p(3 \times 3)$ -3CO; 0.375 ML, $c(4 \times 2)$ -3CO; 0.5 ML, $c(4 \times 2)$ -4CO; 0.58 ML, $(2\sqrt{3} \times 2\sqrt{3})R30^\circ$ -7CO; 0.6 ML, $c(\sqrt{3} \times 5)$ rect-6CO; 0.625 ML, $c(4 \times 2)$ -5CO; 0.67 ML, $c(\sqrt{3} \times 3)$ rect-4CO; 1 ML, $c(4 \times 2)$ -8CO. Four stable ordered stable structures are identified: $(\sqrt{3} \times \sqrt{3})R30^\circ$ -CO, $c(4 \times 2)$ -4CO, $c(\sqrt{3} \times 5)$ rect-6CO, and $c(\sqrt{3} \times 3)$ rect-4CO.

any value of the chemical potential. This is consistent with the experimental surface science data; those intermediate coverage structures have not been observed. The next stable ordered structure is the $c(\sqrt{3} \times 5)$ rect-6CO structure with a coverage of 0.6 ML. The $(2\sqrt{3} \times 2\sqrt{3})R30^\circ$ -7CO structure that is observed on Co(0001), Ru(0001), and Ir(111) is not stable on Pt(111) for any value of the CO chemical potential and has also not been observed experimentally. The next structure is $c(\sqrt{3} \times 3)$ rect-4CO, corresponding to a 0.67 ML coverage. At sufficiently high CO chemical potential, the 1 ML structure is the most stable, but at 300 K, this is only possible at unrealistic CO pressures. It is remarkable that the vdW-DF thermodynamic calculations not only correctly identify the most stable structure for a particular coverage, in particular the change in the bridge:top ratio with coverage, but also correctly identify the ordered structures that are observable and the ordered structures that are not observable on Pt(111), such as $(2\sqrt{3} \times 2\sqrt{3})R30^\circ$ -7CO, $c(4 \times 2)$ -3CO, and $c(4 \times 2)$ -5CO.

The stability diagram in Figure 4 can be used to identify the temperature and pressure domain where each of the four ordered structures is the most stable (Figure 5). At a pressure of 1 bar, the $c(\sqrt{3} \times 5)$ rect-6CO structure (0.67 ML) is the most stable up to 366 K. Above 366 K, some CO desorbs to form the $c(\sqrt{3} \times 5)$ rect-6CO structure. Above 590 K, further CO desorption leads to the $c(4 \times 2)$ -4CO structure and eventually, at 847 K, to the $(\sqrt{3} \times \sqrt{3})R30^\circ$ -CO structure. CO adsorption becomes endergonic at 1010 K (dotted line in Figure 5). Under UHV conditions (10^{-9} mbar), these transitions occur at 180 , 275 , 400 , and 450 K. The transition temperature is sensitive to the calculated reaction enthalpy and entropy. Indeed, at 300 K a 10 kJ/mol change in the differential CO adsorption enthalpy shifts the transition pressure by a factor of 60 , while a 10 J/(mol K) change in

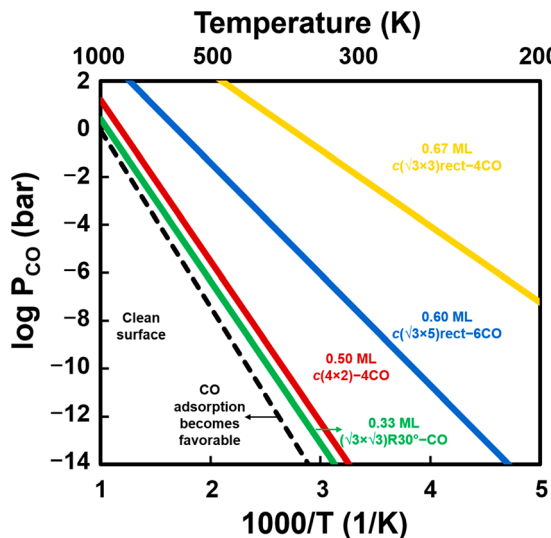


Figure 5. First-principles stability diagram for CO adsorption on Pt(111), showing the stability domains for the four ordered structures that were identified in Figure 4: ($\sqrt{3} \times \sqrt{3}$)R30°-CO, $c(4 \times 2)$ -4CO, $c(\sqrt{3} \times 5)$ rect-6CO, $c(\sqrt{3} \times 3)$ rect-4CO.

the differential adsorption entropy shifts the transition pressure by a factor of 4. Considering their importance to catalysis, the four ordered high-coverage structures that emerge from the stability diagram should be considered in future benchmark studies.

4.5. Change in Bridge:Top Ratio with Coverage. The calculations show a remarkable shift in the site preference with coverage, from top to bridge and back to top, in agreement with experiments. Although only four thermodynamically stable ordered structures corresponding to specific coverages were identified in the calculations, we can computationally evaluate the most stable structure for every possible coverage. For this, we computed the most stable structure for the adsorption of 1 up to 16 CO molecules in a $p(4 \times 4)$ unit cell (Supporting Information, Table S7). For each coverage, various structures with different bridge:top ratios and different relative CO positions were considered. In total, about 150 structures were evaluated. Figure 6 shows how the bridge:top ratio for the most stable structure for a given coverage changes with the CO coverage. In addition, the four stable structures identified in the first-principles stability diagram are indicated in Figure 6. Up to four CO molecules in the $p(4 \times 4)$ unit cell (0.25 ML), CO adsorbs only at the top site in the most stable configuration. For the fifth CO molecule (0.31 ML), adsorption at the bridge sites becomes preferred. The sixth, seventh, and eighth CO molecules also adsorb at the bridge site, and the bridge:top ratio gradually increases with coverage. The transition from top to bridge at ~ 0.3 ML in the $p(4 \times 4)$ unit cell is in line with the stable ($\sqrt{3} \times \sqrt{3}$)R30°-CO structure, the highest coverage structure where CO adsorbs at top sites. Since the ($\sqrt{3} \times \sqrt{3}$)R30°-CO unit cell is not commensurate with the $p(4 \times 4)$ unit cell, the transition from top to bridge happens at a slightly different coverage in the $p(4 \times 4)$ unit cell. The decrease in preference for the top site with coverage was also found in the $p(3 \times 3)$ unit cell (see section 4.1).

Interestingly, the preference for the bridge sites decreases again above 0.5 ML, and from the ninth CO onward the top site is favored. Above 0.5 ML, the bridge:top ratio hence

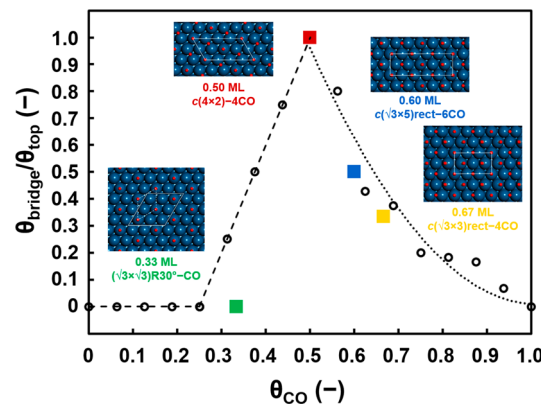


Figure 6. Bridge:top ratio ($\theta_{\text{bridge}}/\theta_{\text{top}}$) for the most stable structure in a $p(4 \times 4)$ unit cell as a function of the total CO coverage (θ_{CO}). Sixteen different coverages were evaluated in the $p(4 \times 4)$ unit cell (Supporting Information, Table S7). The stable ordered structures that were identified in section 4.3 are also indicated: (green ■) ($\sqrt{3} \times \sqrt{3}$)R30°-CO; (red ■) $c(4 \times 2)$ -4CO; (blue ■) $c(\sqrt{3} \times 5)$ rect-6CO; (yellow ■) $c(\sqrt{3} \times 3)$ rect-4CO. Since the unit cells of the ordered structures are not commensurate with the $p(4 \times 4)$ unit cell, the ordered structures do not precisely follow the trend for the $p(4 \times 4)$ unit cell. The data points corresponding to $\theta_{\text{bridge}}/\theta_{\text{top}}$ ratio for $p(4 \times 4)$ unit cell are connected by a dotted line for visual guidance.

decreases, and at 1 ML coverage, the top sites are strongly preferred over the bridge sites. The two stable high-coverage ordered structures, $c(\sqrt{3} \times 5)$ rect-6CO and $c(\sqrt{3} \times 3)$ rect-4CO, follow the trend calculated for the $p(4 \times 4)$ unit cell, even though their unit cell is not commensurate with the $p(4 \times 4)$ unit cell.

In our previous work,²⁵ we showed that the CO site preference is driven by the Pt surface charge, which determines the balance between donation from the CO 5σ orbital to the partially filled Pt states and back-donation from the filled Pt states to the empty CO $2\pi^*$ orbitals. Since back-donation plays a larger role for the bridge site, adsorption at the bridge site is less charge sensitive.²⁵ When CO adsorbs at the top site, charge transfer from CO to surface Pt atoms results in a charge redistribution on the Pt surface, leading to a higher electron density at neighboring empty surface Pt atoms. The increased charge at the neighboring Pt atoms destabilizes CO adsorption at the top site more than adsorption at the bridge site.²⁵ Above a coverage of ~ 0.3 ML, the only available adsorption sites are next to an occupied Pt atom, and adsorption at the bridge sites is preferred. The higher back-donation at the bridge site results in charge transfer from surface Pt atoms to CO and reduces the Pt surface charge. This reverses the CO adsorption site preference from bridge back to top for coverages above 0.5 ML.

5. CONCLUSIONS

The adsorption of CO on Pt(111) was studied using thermodynamic vdW-DF density functional theory. Several hundred possible adsorption structures were evaluated computationally, where CO adsorbs at top, bridge, and hollow sites. Out of the many possible structures, four stable ordered structures were identified: a 0.33 ML ($\sqrt{3} \times \sqrt{3}$)R30°-CO structure with CO at top sites, a 0.5 ML $c(4 \times 2)$ -4CO structure with equal population of top and bridge sites, a 0.60 ML $c(\sqrt{3} \times 5)$ rect-6CO structure with a bridge:top ratio of 1:2, and a 0.67 ML $c(\sqrt{3} \times 3)$ rect-4CO structure with a

bridge:top ratio of 1:3, the saturation coverage. Other ordered structures, for example the $(2\sqrt{3} \times 2\sqrt{3})R30^\circ$ -7CO structure observed on other surfaces, were not stable for any value of the CO chemical potential. Remarkably, these four structures calculated by vdW-DF correspond with the only four structures that have been reported in the large body of surface science literature for CO on Pt(111). For the high-coverage structures, several structures can be found in the literature, and the DFT calculations can help to settle this debate. The calculations can furthermore be used to identify the most stable structure for a given coverage, even for coverages that do not correspond to a stable ordered structure. This allowed us to evaluate the change in site preference, from top to bridge and back to top, as a function of coverage. The $(\sqrt{3} \times \sqrt{3})R30^\circ$ -CO structure is the highest coverage structure where CO adsorbs at top sites. The repulsive interaction between the CO 5σ orbital and the Pt states increases the electron density at neighboring Pt atoms which favors bridge adsorption at these sites, up to 0.5 ML. Above this coverage, the higher back-donation at the bridge sites decreases the Pt charge, which favors top adsorption.

ASSOCIATED CONTENT

Supporting Information

The Supporting Information is available free of charge on the ACS Publications website at DOI: [10.1021/acscatal.8b02371](https://doi.org/10.1021/acscatal.8b02371).

Equations used to calculate average and differential adsorption energy, Gibbs free adsorption energy, and CO chemical potential, possible CO adsorption sites and frequency modes on a Pt catalyst surface, average CO adsorption energies, average Gibbs free adsorption energies (kJ/mol), and average entropy of adsorbed CO for different CO coverages and configurations obtained with vdW-DF, PBE functionals for $p(3 \times 3)$, $c(4 \times 2)$, $c(\sqrt{3} \times 2)\text{rect}$, $c(\sqrt{3} \times 5)\text{rect}$, $c(\sqrt{3} \times 3)\text{rect}$, and $p(4 \times 4)$ unit cells, and vdW-DF frequencies of adsorbed CO for different configurations and coverages ([PDF](#))

AUTHOR INFORMATION

Corresponding Author

*E-mail for M.S.: mark.saeys@ugent.be.

ORCID

G. T. Kasun Kalhaba Gunasooriya: [0000-0003-1258-7841](#)

Mark Saeys: [0000-0002-3426-6662](#)

Notes

The authors declare no competing financial interest.

ACKNOWLEDGMENTS

This work was supported by an Odysseus grant from the Research Foundation-Flanders (No. FWO G0E5714N). The computational resources (Stevin Supercomputer Infrastructure) and services used in this work were provided by the VSC (Flemish Supercomputer Center), funded by Ghent University, FWO, and the Flemish Government, department EWI.

REFERENCES

- Chorkendorff, I.; Niemantsverdriet, J. W. Concepts of Modern Catalysis and Kinetics. In *Concepts of Modern Catalysis and Kinetics*, 2nd ed.; Wiley-VCH: 2003.
- Allian, A. D.; Takanabe, K.; Fujidala, K. L.; Hao, X.; Truex, T. J.; Cai, J.; Buda, C.; Neurock, M.; Iglesia, E. Chemisorption of CO and Mechanism of CO Oxidation on Supported Platinum Nanoclusters. *J. Am. Chem. Soc.* **2011**, *133*, 4498–4517.
- Chua, Y. P. G.; Gunasooriya, G. T. K. K.; Saeys, M.; Seebauer, E. G. Controlling the CO oxidation rate over Pt/TiO₂ catalysts by defect engineering of the TiO₂ support. *J. Catal.* **2014**, *311*, 306–313.
- Fu, Q.; Saltsburg, H.; Flytzani-Stephanopoulos, M. Active Nonmetallic Au and Pt Species on Ceria-Based Water-Gas Shift Catalysts. *Science* **2003**, *301*, 935–938.
- Rodriguez, J. A.; Ma, S.; Liu, P.; Hrbek, J.; Evans, J.; Perez, M. Activity of CeO_x and TiO_x nanoparticles grown on Au(111) in the water-gas shift reaction. *Science* **2007**, *318*, 1757–1760.
- Khodakov, A. Y.; Chu, W.; Fongarland, P. Advances in the Development of Novel Cobalt Fischer-Tropsch Catalysts for Synthesis of Long-Chain Hydrocarbons and Clean Fuels. *Chem. Rev.* **2007**, *107*, 1692–1744.
- den Breejen, J. P.; Radstake, P. B.; Bezemer, G. L.; Bitter, J. H.; Frøseth, V.; Holmen, A.; Jong, K. P. d. On the Origin of the Cobalt Particle Size Effects in Fischer-Tropsch Catalysis. *J. Am. Chem. Soc.* **2009**, *131*, 7197–7203.
- Gunasooriya, G. T. K. K.; van Bavel, A. P.; Kuipers, H. P. C. E.; Saeys, M. Key Role of Surface Hydroxyl Groups in C–O Activation during Fischer-Tropsch Synthesis. *ACS Catal.* **2016**, *6*, 3660–3664.
- Santen, R. A. Heterogeneous Catalysis. In *Modern Heterogeneous Catalysis*; Wiley-VCH: 2017; pp 15–58.
- Langmuir, I. The mechanism of the catalytic action of platinum in the reactions $2\text{CO} + \text{O}_2 = 2\text{CO}_2$ and $2\text{H}_2 + \text{O}_2 = 2\text{H}_2\text{O}$. *Trans. Faraday Soc.* **1922**, *17*, 621–654.
- Ertl, G. Basic Principles. In *Reactions at Solid Surfaces*; Wiley: 2010; pp 1–19.
- Papp, H. The chemisorption of carbon monoxide on a Co(0001) single crystal surface; studied by LEED, UPS, EELS, AES and work function measurements. *Surf. Sci.* **1983**, *129*, 205–218.
- Pfnür, H.; Menzel, D.; Hoffmann, F. M.; Ortega, A.; Bradshaw, A. M. High resolution vibrational spectroscopy of CO on Ru(001): The importance of lateral interactions. *Surf. Sci.* **1980**, *93*, 431–452.
- Avery, N. R. Electron energy loss spectroscopic study of CO on Pt(111). *J. Chem. Phys.* **1981**, *74*, 4202–4203.
- Persson, B. N. J.; Tüshaus, M.; Bradshaw, A. M. On the nature of dense CO adlayers. *J. Chem. Phys.* **1990**, *92*, 5034–5046.
- Petrova, N. V.; Yakovkin, I. N. Lateral interaction and CO adlayer structures on the Pt(111) surface. *Surf. Sci.* **2002**, *519*, 90–100.
- Feibelman, P. J.; Hammer, B.; Nørskov, J. K.; Wagner, F.; Scheffler, M.; Stumpf, R.; Watwe, R.; Dumesic, J. The CO/Pt(111) Puzzle. *J. Phys. Chem. B* **2001**, *105*, 4018–4025.
- Kresse, G.; Gil, A.; Sautet, P. Significance of single-electron energies for the description of CO on Pt(111). *Phys. Rev. B: Condens. Matter Mater. Phys.* **2003**, *68*, 073401.
- Hu, Q.-M.; Reuter, K.; Scheffler, M. Towards an Exact Treatment of Exchange and Correlation in Materials: Application to the "CO Adsorption Puzzle" and Other Systems. *Phys. Rev. Lett.* **2007**, *98*, 176103.
- Schimka, L.; Harl, J.; Stroppa, A.; Grüneis, A.; Marsman, M.; Mittendorfer, F.; Kresse, G. Accurate surface and adsorption energies from many-body perturbation theory. *Nat. Mater.* **2010**, *9*, 741–744.
- Gautier, S.; Steinmann, S. N.; Michel, C.; Fleurat-Lessard, P.; Sautet, P. Molecular adsorption at Pt(111). How accurate are DFT functionals? *Phys. Chem. Chem. Phys.* **2015**, *17*, 28921–28930.
- Steckel, J. A.; Eichler, A.; Hafner, J. CO adsorption on the CO-precovered Pt(111) surface characterized by density-functional theory. *Phys. Rev. B: Condens. Matter Mater. Phys.* **2003**, *68*, 085416.
- Shan, B.; Zhao, Y.; Hyun, J.; Kapur, N.; Nicholas, J. B.; Cho, K. Coverage-Dependent CO Adsorption Energy from First-Principles Calculations. *J. Phys. Chem. C* **2009**, *113*, 6088–6092.
- Dimakis, N.; Navarro, N. E.; Mion, T.; Smotkin, E. S. Carbon Monoxide Adsorption Coverage Study on Platinum and Ruthenium Surfaces. *J. Phys. Chem. C* **2014**, *118*, 11711–11722.

- (25) Gunasooriya, G. T. K. K.; Saeys, M. CO Adsorption Site Preference on Platinum: Charge Is the Essence. *ACS Catal.* **2018**, *8*, 3770–3774.
- (26) Shigeishi, R. A.; King, D. A. Chemisorption of carbon monoxide on platinum {111}: Reflection-absorption infrared spectroscopy. *Surf. Sci.* **1976**, *58*, 379–396.
- (27) Crossley, A.; King, D. A. Infrared spectra for co isotopes chemisorbed on Pt “111”: Evidence for strong adsorbate coupling interactions. *Surf. Sci.* **1977**, *68*, 528–538.
- (28) Ertl, G.; Neumann, M.; Streit, K. M. Chemisorption of CO on the Pt(111) surface. *Surf. Sci.* **1977**, *64*, 393–410.
- (29) Hopster, H.; Ibach, H. Adsorption of CO on Pt(111) and Pt 6(111) × (111) studied by high resolution electron energy loss spectroscopy and thermal desorption spectroscopy. *Surf. Sci.* **1978**, *77*, 109–117.
- (30) Steininger, H.; Lehwald, S.; Ibach, H. On the adsorption of CO on Pt(111). *Surf. Sci.* **1982**, *123*, 264–282.
- (31) Heyden, B. E.; Bradshaw, A. M. The adsorption of CO on Pt(111) studied by infrared reflection—Absorption spectroscopy. *Surf. Sci.* **1983**, *125*, 787–802.
- (32) Biberian, J. P.; Van Hove, M. A. A new model for CO ordering at high coverages on low index metal surfaces: A correlation between LEED, HREELS and IRS: II. CO adsorbed on fcc (111) and hep (0001) surfaces. *Surf. Sci.* **1984**, *138*, 361–389.
- (33) Tüshaus, M.; Schweizer, E.; Hollins, P.; Bradshaw, A. M. Yet another vibrational study of the adsorption system Pt{111}-CO. *J. Electron Spectrosc. Relat. Phenom.* **1987**, *44*, 305–316.
- (34) Kiskinova, M.; Szab, A.; Yates, J. T., Jr Compressed CO overlayers on Pt(111) - Evidence for tilted CO species at high coverages by digital ESDIAD. *Surf. Sci.* **1988**, *205*, 215–229.
- (35) Schweizer, E.; Persson, B. N. J.; Tüshaus, M.; Hoge, D.; Bradshaw, A. M. The potential energy surface, vibrational phase relaxation and the order-disorder transition in the adsorption system Pt{111}-CO. *Surf. Sci.* **1989**, *213*, 49–89.
- (36) Brown, W. A.; Kose, R.; King, D. A. Femtomole Adsorption Calorimetry on Single-Crystal Surfaces. *Chem. Rev.* **1998**, *98*, 797–832.
- (37) Lee, W. T.; Ford, L.; Blowers, P.; Nigg, H. L.; Masel, R. I. Why do heats of adsorption of simple gases on platinum surfaces vary so little with surface structure? *Surf. Sci.* **1998**, *416*, 141–151.
- (38) Yang, H. J.; Minato, T.; Kawai, M.; Kim, Y. STM Investigation of CO Ordering on Pt(111): From an Isolated Molecule to High-Coverage Superstructures. *J. Phys. Chem. C* **2013**, *117*, 16429–16437.
- (39) Fischer-Wolfsberg, J. H.; Hartmann, J.; Farmer, J. A.; Flores-Camacho, J. M.; Campbell, C. T.; Schauermann, S.; Freund, H. J. An improved single crystal adsorption calorimeter for determining gas adsorption and reaction energies on complex model catalysts. *Rev. Sci. Instrum.* **2011**, *82*, 024102.
- (40) Yeo, Y. Y.; Vattuone, L.; King, D. A. Calorimetric heats for CO and oxygen adsorption and for the catalytic CO oxidation reaction on Pt{111}. *J. Chem. Phys.* **1997**, *106*, 392–401.
- (41) Lahee, A. M.; Toennies, J. P.; Wöll, C. Low energy adsorbate vibrational modes observed with inelastic helium atom scattering: CO on Pt(111). *Surf. Sci.* **1986**, *177*, 371–388.
- (42) Björneholm, O.; Nilsson, A.; Tillborg, H.; Bennich, P.; Sandell, A.; Hernnäs, B.; Puglia, C.; Mårtensson, N. Overlayer structure from adsorbate and substrate core level binding energy shifts: CO, CCH₃ and O on Pt(111). *Surf. Sci.* **1994**, *315*, L983–L989.
- (43) Dion, M.; Rydberg, H.; Schröder, E.; Langreth, D. C.; Lundqvist, B. I. Van der Waals density functional for general geometries. *Phys. Rev. Lett.* **2004**, *92*, 246401.
- (44) Klimeš, J.; Bowler, D. R.; Michaelides, A. Van der Waals density functionals applied to solids. *Phys. Rev. B: Condens. Matter Mater. Phys.* **2011**, *83*, 195131.
- (45) Kresse, G.; Furthmüller, J. Efficient iterative schemes for ab initio total-energy calculations using a plane-wave basis set. *Phys. Rev. B: Condens. Matter Mater. Phys.* **1996**, *54*, 11169.
- (46) Kresse, G.; Furthmüller, J. Efficiency of ab-initio total energy calculations for metals and semiconductors using a plane-wave basis set. *Comput. Mater. Sci.* **1996**, *6*, 15.
- (47) Perdew, J. P.; Burke, K.; Ernzerhof, M. Generalized Gradient Approximation Made Simple. *Phys. Rev. Lett.* **1996**, *77*, 3865.
- (48) Wyckoff, R. W. G. *Crystal Structures*; Krieger Publishing: Malabar, FL, 1982; Vol. 1.
- (49) Makov, G.; Payne, M. C. Periodic boundary conditions in ab initio calculations. *Phys. Rev. B: Condens. Matter Mater. Phys.* **1995**, *51*, 4014–4022.
- (50) Smith, J. M.; Van Ness, H. C.; Abbott, M. M. *Introduction to Chemical Engineering Thermodynamics*, 6th ed.; McGraw Hill: New York, 2001; pp 353.
- (51) Sprowl, L. H.; Campbell, C. T.; Árnadóttir, L. Hindered Translator and Hindered Rotor Models for Adsorbates: Partition Functions and Entropies. *J. Phys. Chem. C* **2016**, *120*, 9719–9731.
- (52) Kinne, M.; Fuhrmann, T.; Whelan, C. M.; Zhu, J. F.; Pantförder, J.; Probst, M.; Held, G.; Denecke, R.; Steinrück, H.-P. Kinetic parameters of CO adsorbed on Pt(111) studied by in situ high resolution x-ray photoelectron spectroscopy. *J. Chem. Phys.* **2002**, *117*, 10852–10859.
- (53) Gunasooriya, G. T. K. K.; van Bavel, A. P.; Kuipers, H. P. C. E.; Saeys, M. CO adsorption on cobalt: Prediction of stable surface phases. *Surf. Sci.* **2015**, *642*, L6–L10.
- (54) Weststrate, C. J.; van de Loosdrecht, J.; Niemantsverdriet, J. W. Spectroscopic insights into cobalt-catalyzed Fischer–Tropsch synthesis: A review of the carbon monoxide interaction with single crystalline surfaces of cobalt. *J. Catal.* **2016**, *342*, 1–16.
- (55) Yeo, Y. Y.; Stuck, A.; Wartnaby, C. E.; King, D. A. Microcalorimetric study of ethylene adsorption on the Pt{111} surface. *Chem. Phys. Lett.* **1996**, *259*, 28–36.
- (56) Lauterbach, J.; Boyle, R. W.; Schick, M.; Mitchell, W. J.; Meng, B.; Weinberg, W. H. The adsorption of CO on Ir(111) investigated with FT-IRAS. *Surf. Sci.* **1996**, *350*, 32–44.